Matter

CellPress
OPEN ACCESS

Article

Porous bulk superhydrophobic nanocomposites for extreme environments

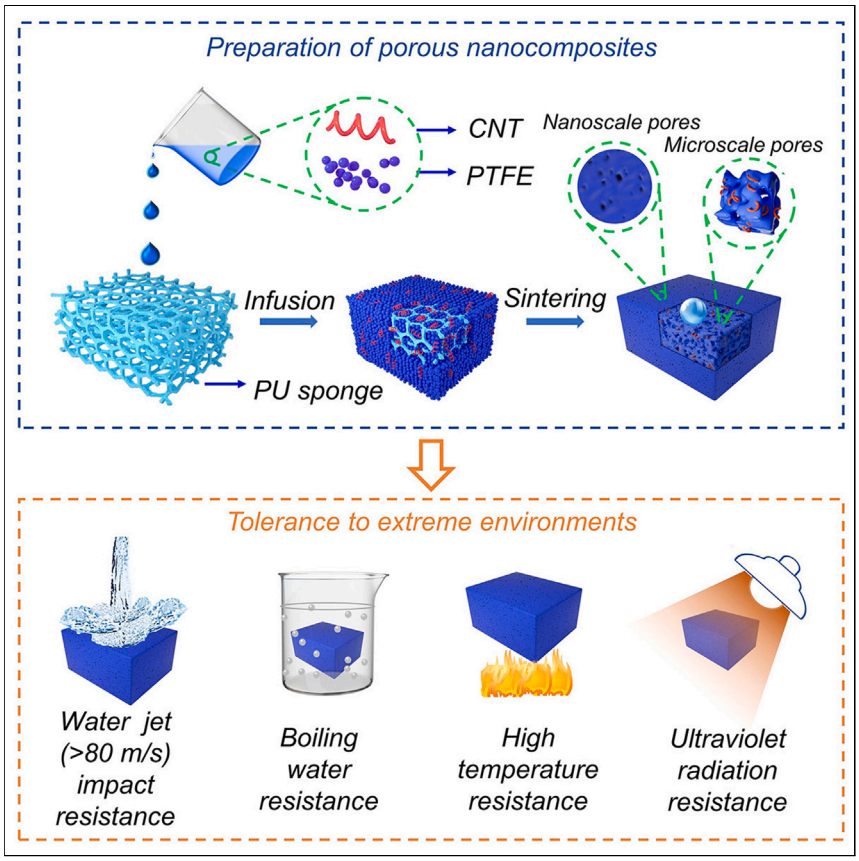

Novel porous CNT/PTFE nanocomposites were developed as bulk superhydrophobic materials for extreme environments. The nanocomposite could resist high-speed water jets (>80 m s^{-1}), immersion in boiling water, and exposure to high temperature and ultraviolet light and showed excellent icephobicity. The nanocomposites were also mechanically robust and could be designed into machinable shapes and sizes. They should find applications in, for example, infrastructure components exposed to the elements, the chemical industry, and corrosion protection.

Binrui Wu, Yunyun Meng, Chaoyi Peng, ..., Jun Yang, Shuxin Bai, Manish K. Tiwari

chaoyi.peng@foxmail.com (C.P.)
lierenwn@nudt.edu.cn (N.W.)
m.tiwari@ucl.ac.uk (M.K.T.)

Highlights

Constructing robust superhydrophobic nanocomposites with a hierarchal porosity

Realizing superhydrophobic nanocomposite with resistance to extreme environments

Resisting to liquid jet impacts at >85 m s^{-1} without losing superhydrophobicity

1 **Discovery**
A new material or phenomena

Wu et al., Matter 6, 1–13
June 7, 2023
https://doi.org/10.1016/j.matt.2023.03.033

Please cite this article in press as: Wu et al., Porous bulk superhydrophobic nanocomposites for extreme environments, Matter (2023), https://doi.org/10.1016/j.matt.2023.03.033

Matter

CellPress
OPEN ACCESS

Article

Porous bulk superhydrophobic nanocomposites for extreme environments

Binrui Wu,[1,2,6,7] Yunyun Meng,[1,7] Chaoyi Peng,[1,3,*] Jinshui Yang,[1] Suli Xing,[1] Nan Wu,[1,*] Changping Yin,[1] Jun Yang,[3] Shuxin Bai,[1] and Manish K. Tiwari[4,5,8,*]

SUMMARY

Robust superhydrophobic materials providing protections from harsh weather events such as hurricanes, high temperatures, and humid/frigid conditions have proven challenging to achieve. Here, we report a porous bulk nanocomposite comprising carbon nanotube (CNT)-reinforced polytetrafluoroethylene (PTFE). The nanocomposites are prepared using a templated approach by infusing a CNT/PTFE dispersion into a sponge followed by thermal annealing and decomposition of the sponge template. Importantly, an excess accretion of CNT/PFFE particle mixture on the sponge resulted in nanocomposites with unique and hierarchical porous microstructure, featuring nanochannels near the surface connected to microscale pores inside. The superhydrophobic nanocomposite could resist liquid jets impacting at a velocity of ~85.4 m s^{-1} (Weber number of ~202,588) and exhibits excellent high-temperature resistance as well as mechanochemical robustness. The porous nanocomposites display excellent icephobicity both with and without infusion with polydimethylsiloxane/silicone oil. These properties should facilitate exploitation as stiff/strong structural polymeric foams used in a variety of fields.

INTRODUCTION

Bioinspired superhydrophobic surfaces have a static water drop contact angle (θ) greater than 150°, roll-off/sliding angle (θ_s) less than 10°,[1,2] and rely on a combination of low-surface-energy materials and surface texture designs to achieve these wetting properties. Such surfaces have a wide range of possible applications. For example, superhydrophobic materials (including coatings, fabrics, and bulk components) with good abrasion resistance, chemical resistance, and impact resistance (e.g., impacts by solid particles and/or water drops/jets) have been reported. A key challenge is mechanical fragility of asperities, which are part of the surface texture, and resistance to impalement by dynamic liquid menisci (e.g., those appearing during impact of liquids on surfaces). Wang et al.[3] developed a strategy to enhance robustness of superhydrophobic coating by protecting the fragile micro-/nanoscale structures using microscale armor. We reported an all-organic superhydrophobic material formulation that could sustain liquid impacts at 35 m s^{-1} and also offered multi-faceted mechanochemical robustness.[4] However, for harsh weather or extreme industrial conditions, these may still prove inadequate. For example, in a category 5 hurricane, the surface/material is exposed to liquid impacts at >70 m s^{-1}. High-speed transport vehicles, unmanned aerial vehicles, and wind turbine blades are also routinely exposed water/raindrops with speeds >70 m s^{-1}, and the related erosion protection is a major bottleneck in these applications.

PROGRESS AND POTENTIAL

Superhydrophobic surfaces possess many fascinating properties. Unfortunately, despite progress, the durability required for extreme environments has remained a challenge. In this work, we develop porous bulk nanocomposites featuring superficial nanochannels connected to microscale pores inside. The unique hierarchical porous structures and mechanochemical robustness of the nanocomposites enable resistance to various mechanical/chemical/thermal/icing/radiation tests as well as liquid impacts at >80 m s^{-1}. Such all-around robustness should inspire new applications of superhydrophobic materials in extreme environments.

Please cite this article in press as: Wu et al., Porous bulk superhydrophobic nanocomposites for extreme environments, Matter (2023), https://doi.org/10.1016/j.matt.2023.03.033

Flexibility and fine nanostructures are effective ways to help superhydrophobic surfaces to resist liquid impact. Inspired by butterflies, Vasileiou et al.[5] found that flexibility can work synergistically with hierarchical surface morphology and improve water drop impalement resistance of the surface. However, such unsupported, flexible surfaces inspired by butterfly wings are unlikely to be suitable for bulk components. Luo et al.[6] developed a transparent poly(ethylene-co-acrylic acid)/SiO_2 coating with nanoaggregates; the fine texture enabled resistance to water impacts up to ~15 m s^{-1}. Even a combination of fine textures with flexibility may struggle in harsh conditions. Thus, while these prior works are encouraging, they fall well short of being able to sustain the high dynamic impact pressures engendered by liquid impacts of over 70 m s^{-1}, which is a daunting challenge.

Additionally, a number of applications involve exposure to thermal cycles, hot steam (e.g., components in steam condensers),[7] high-temperature chemical processing, and/or hot and humid environments.[8,9] These applications demand thermal stability.[10,11] Furthermore, hot water resistance is also critical when exposing superhydrophobic surfaces to hot or even boiling water conditions. The hot water vapor can condense into the microstructures of superhydrophobic surfaces, resulting in Cassie-to-Wenzel transition that significantly increases adhesion of water to the surfaces.[12] Polymer-based objects tend to be flammable, which limits their range of applications. Thus, thermal stability and appropriate heat dissipation are necessary in designing fire-resistant materials. Similarly, ice accretion is another extreme challenge that superhydrophobic materials are often expected to address. Finally, several outdoor applications demand resistance against UV irradiation.[3]

We conceived several strategies to address these challenges. Our first strategy is to build nanochannels (pores) on the surface in order to enhance the resistive capillary pressure against impinging liquid meniscus.[13] In fact, the smaller the pore size, better the impact resistance.[14] The capillary pressure from the nanochannels must resist the compressive water hammer pressure (P_{WH})[4] (relevant at higher impact velocities). Thus, as a second strategy, we use hydrophobic materials with low acoustic impedance to reduce the P_{WH} peaks and improve the liquid impact resistance. The third strategy is to use hydrophobic materials with low surface energy and high melting point; the latter makes perfluorinated silanes—a common practice in the literature—unsuitable. We selected PTFE as the main ingredient, owing to its lowest surface energy among solid materials as well as better thermal performance compared with other hydrophobic polymers such as polydimethylsiloxane, polystyrene, and polyvinylidene fluoride.[15] Additionally, its acoustic impedance is one-quarter that of inorganic materials such as silica (a common ingredient in superhydrophobic materials), leading to lower P_{WH} peaks. However, poor solution processability and, more importantly, the mechanical properties of PTFE are limitations. Therefore, CNT was used as reinforcement. The CNT/PTFE combination is not new, and a few previous studies have used it. For example, Zhu et al.[16] fabricated superhydrophobic bulk components by compressing a mixture of PTFE and CNT. Donati et al.[17] prepared a superhydrophobic coating by spraying CNT/PTFE suspension followed by thermal annealing. Unfortunately, neither approach is suitable for controlling the pore sizes in the final nanocomposite. The compression process consolidates the particles together, while spraying/annealing results in self-assembly of particles into clusters with resulting pores of ~1-μm scale. Finer nanoscale pores will be more desirable for better liquid impalement resistance. This is the primary reason why none of the aforementioned materials could attain the kind of robustness we report here.

[1]Department of Materials Science and Engineering, College of Aerospace Science and Engineering, National University of Defense Technology, Changsha, Hunan 410073, P.R. China

[2]State Key Laboratory of NBC Protection for Civilian, Beijing 102205, P.R. China

[3]Zhuzhou Times New Materials Technology Co., Ltd, Zhuzhou, Hunan 412007, P.R. China

[4]Nanoengineered Systems Laboratory, UCL Mechanical Engineering, University College London, Torrington Place, WC1E 7JE London, UK

[5]Wellcome/EPSRC Centre for Interventional and Surgical Sciences (WEISS), University College London, W1W 7TS London, UK

[6]China Aerodynamics Research and Development Center, Mianyang, Sichuan 621000, P.R. China

[7]These authors contributed equally

[8]Lead contact

*Correspondence: chaoyi.peng@foxmail.com (C.P.), lierenwn@nudt.edu.cn (N.W.), m.tiwari@ucl.ac.uk (M.K.T.)

https://doi.org/10.1016/j.matt.2023.03.033

Please cite this article in press as: Wu et al., Porous bulk superhydrophobic nanocomposites for extreme environments, Matter (2023), https://doi.org/10.1016/j.matt.2023.03.033

We introduce a new approach to prepare porous, bulk superhydrophobic nanocomposites with a nanoporous structure on the surface, which is connected to microscale pores inside. We used polyurethane (PU) sponges as templates for controlled impregnation of CNT/PTFE particles. CNT/PTFE mixtures were dispersed in ethanol to impregnate/wet the PU sponge followed by sintering. Importantly, we ensured an excess layer of CNT/PTFE mixture on the sponge template to obtain superficial nanoporosity. Following impregnation and drying, the PU sponge was removed through thermal degradation. The resulting bulk and nanoporous nanocomposites featured nanoscale channels on the surface and microporosity in the bulk (with associated variations in mechanical stiffness). This hierarchical porosity combined with robustness of the nanocomposites enabled them to sustain water jets up to a speed of ~85.4 m s^{-1}. Interestingly, the nanopores on the surface and the larger pores in bulk also enabled spontaneous dislodging/ejection of any impaled water through capillary action, which we established through high-speed imaging and analysis of the liquid ejection timescale. By altering the shape/size of the sponge template we were able to alter the shape/size of the superhydrophobic nanocomposites. Additionally, these nanocomposites show excellent mechanochemical robustness, thermal stability, and fire retardancy, benefiting from stability of the PTFE/CNT mixture, and are icephobic. The icephobicity can be further enhanced by inclusion of soft silicones into the porous structure. Overall, the nanocomposite bulks demonstrate significant all-round robustness derived from our fabrication strategy and choice of nanoparticles.

RESULTS AND DISCUSSION

Nanocomposite manufacture

To manufacture the bulk nanocomposites, a PU sponge—acting as template—was immersed multiple times in an ethanol dispersion of CNT and PTFE nanoparticles. Owing to the good wetting ability of ethanol, the mixed nanoparticles readily penetrated the PU sponge pores. Following evaporation of ethanol, the particles adhered to the pore walls. Through multiple impregnation and drying steps, the template was fully loaded, and pores on the surface were filled with nanoparticles. Further immersion with the dispersion led to formation of a CNT/PTFE accretion layer on the surface. This was followed by heating, which led to thermal degradation of the PU backbone, particle sintering, and creation of the nanoporous structure in the accretion layer. The PU sponge template enabled a microporous structure in the interior (see experimental procedures for details, and Figure 1A). The morphology of the superhydrophobic nanocomposites with 12 wt % of CNT is shown in the scanning electron microscopy (SEM) image in Figure 1B. The nanocomposite was observed to be superhydrophobic for all CNT concentrations (see Figure S1A and Note S1). The hierarchical porous structure offers reassurance that our fabrication process is in fact aided and not affected by thermal degradation of the PU foam template (see the thermogravimetric profile for PU foam in Figure S1B). Fourier transform infrared (FTIR) spectroscopy was used to confirm the composition of the final nanocomposite (Figure S1C). The high-magnification SEM image in Figure 1C reveals the nanoscale channels on the surface (i.e., in the accretion layer). Figure 1D shows the morphologies of the accretion layer; clearly the superficial nanochannels are well connected with the microporous structure inside. The nanocomposite was cleaved to image the inner morphology with SEM (Figures S1D and S1E).

The density, compressive strength, and compressive modulus of the nanocomposites were then evaluated for different CNT contents (Figures S2A–S2C and Note S2). As the CNT concentration increased, both compressive strength and

Please cite this article in press as: Wu et al., Porous bulk superhydrophobic nanocomposites for extreme environments, Matter (2023), https://doi.org/10.1016/j.matt.2023.03.033

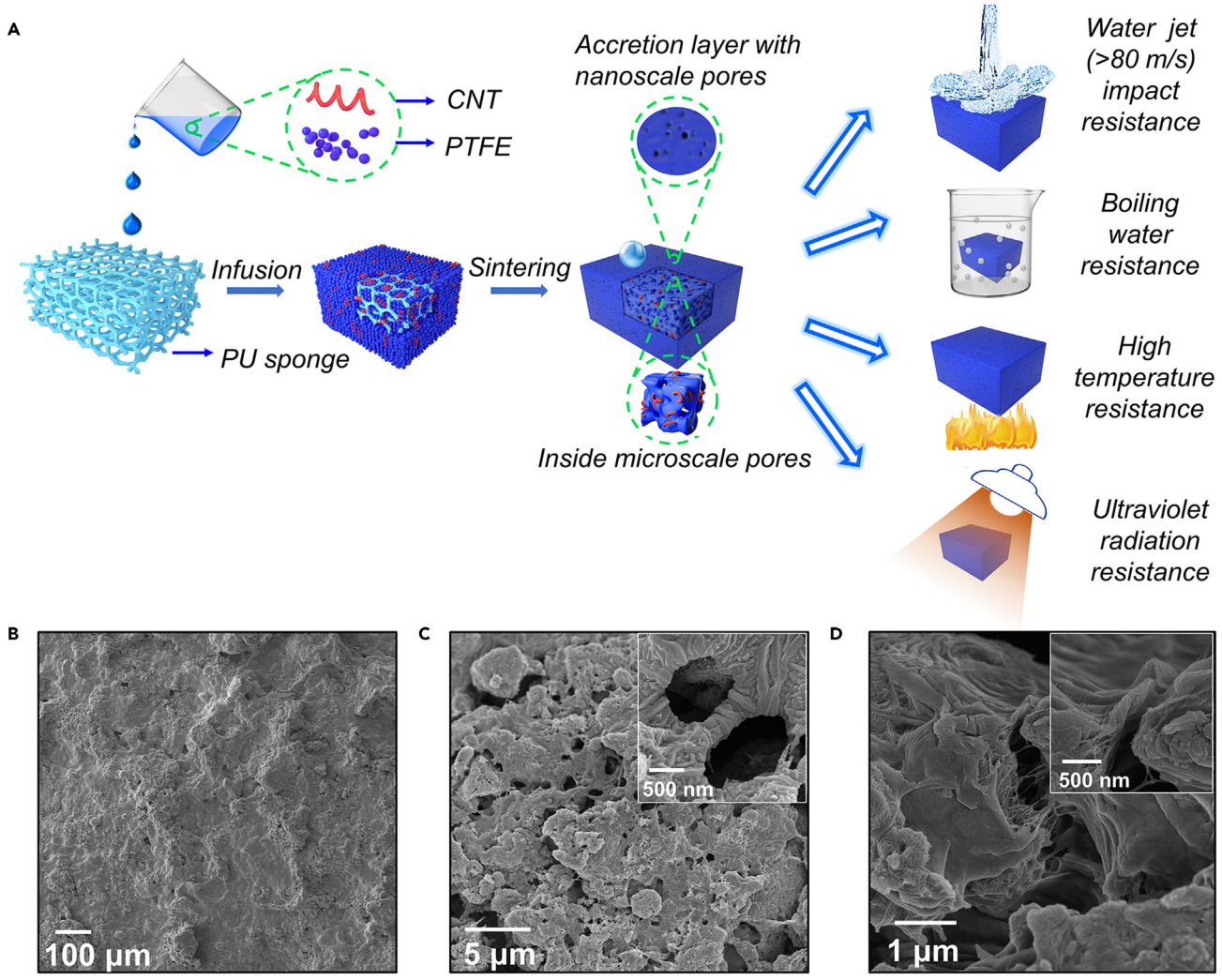

Figure 1. Nanocomposites manufacture and morphology

(A) Fabrication steps for the porous, bulk superhydrophobic nanocomposites, with a hierarchical structure featuring fine pores on the surface connected to microchannels/pores inside.

(B and C) SEM images for the surface parts of the bulk. The inset shows higher-magnification view.

(D) Cross-section SEM images of the larger pores (channels) in the interior of the nanocomposites. The inset shows higher-magnification view, showing the larger channel dimensions.

compressive modulus initially increased, peaking at 8 wt % of CNT, before deteriorating due to CNT agglomeration (Figure S2D). When CNT concentration was increased from 8 to 12 wt %, the specific modulus was reduced by 45% while the specific strength remained nearly the same. The density also reduced slightly (Figures S2A and S2B). A lower density and specific modulus reduce the acoustic impedance of the material, which lowers the peak water hammer pressure during liquid impact and improves impalement resistance.[14] Therefore, the remaining tests were performed with a CNT content of 12 wt %.

High-speed liquid impact resistance

Resistance to dynamic impact and impalement by water drops and jets is essential for superhydrophobic surfaces to suit a variety of applications. For example, during storms or hurricanes, infrastructure components must withstand impact from

Please cite this article in press as: Wu et al., Porous bulk superhydrophobic nanocomposites for extreme environments, Matter (2023), https://doi.org/10.1016/j.matt.2023.03.033

ultra-high-speed water drops. A similar challenge is encountered in the transport sector and with vehicles moving at high speed. To start with, our porous nanocomposites should facilitate drainage of air beneath impacting droplets, which is known to reduce the water hammer pressure of impact. Additionally, the organic constituents are more likely to reduce the acoustic impedance of the material (e.g., 2.9 MRayl for PTFE is only about one-fourth that of silica,[4] and that of CNT is similar[18]). Low acoustic impedance can strongly reduce water hammer pressure and significantly enhance the impact resistance.[4] Thus, we investigated the impact of liquid drops and jets. Figure 2A shows water drops impacting the superhydrophobic nanocomposites at ~4.43 m s^{-1} (obtained by releasing water droplets from 1 m; see also Figure S3A and Videos S1 and S2 for two different drop impact speeds). The drop diameter is 2.37 mm. The water drop undergoes inertial breakage after impact, and each atomized droplet is observed to rebound from the surfaces[19–22] as well.

To investigate higher-speed impacts, a water jet was generated using a commercial high-pressure washer (Figure S3B). We tested the impact resistance of the superhydrophobic nanocomposites up to ~85.4 m s^{-1} using a 2.0-mm jet (Figure 2B and Video S3). This corresponds to a liquid Weber number (We_l) of ~202,588 ($We_l = \rho_l V^2 d/\gamma$, with ρ_l denoting the liquid density, γ the liquid-gas interfacial tension, V the impact speed, and d the characteristic length scale, taken as the diameter for both the jet and drops, with the surface energy of water at room temperature 72.0 mN m^{-1}. To visualize severity of water jet impact tests, an apple, a piece of cardboard, a lotus leaf (a natural superhydrophobic surface, see blue box in Figure 2C), and our nanocomposites were all subjected to the same jet at ~70 m s^{-1} (Video S4). All materials except our sample failed mechanically.

We also observed an intriguing phenomenon after this high-speed jet impact. Directly after the end of the impact test, two water drops on the surface (see red and blue boxes in Figure 2B) grew in the impact area and finally fell off from the surface within ~0.9 s. Essentially the peak impact pressure in the region of jet impact causes impalement into the nanocomposites' pores. Post impact, the hierarchical porous structure helps eject any liquid (the mechanical robustness of the nanocomposite ensures no damage). The dynamics of this ejection are controlled by a balance of capillary, gravity, and viscous forces. A scaling analysis (see Note S3 and the schematic of liquid motion through hydrophobic porous structure in Figure 2D) shows the timescale of liquid ejection as $\tau \sim \frac{\eta h_0^2}{2\gamma R}$, where h_0 is the liquid penetration depth, η and γ are liquid dynamic viscosity and surface tension, and R is the pore radius. Considering h_0 as centimetric (i.e., penetration depth comparable with sample size), we obtain $\tau \sim O(1)$ s for $R \sim 1$ μm and $O(10)$ s for $R \sim 10$ μm (Figure S3C). This compares very well with the drainage time observed in Video S3.

To assess the importance of the fine channel structure on the surface of the nanocomposites, water jet impact tests were also performed on the samples synthesized without the accretion layer (the corresponding surface structure is shown in Figure S1F and differs from the pristine PU sponge morphology shown in Figure S1G). The optical images shown in Figures S1H–S1I also confirm the difference made by the accretion layer. The impact test on a nanocomposite without the superficial nanoporous layer is captured in Video S5. After a brief period of impact at ~28.6 m s^{-1} ($We_l \sim 22{,}721$), the impact area was clearly wetted by the jet. This indicates that the porous structure created solely by the PU sponge template is inadequate for high-speed impact resistance and attests to the merit of the accretion layer used in our fabrication process.

Please cite this article in press as: Wu et al., Porous bulk superhydrophobic nanocomposites for extreme environments, Matter (2023), https://doi.org/10.1016/j.matt.2023.03.033

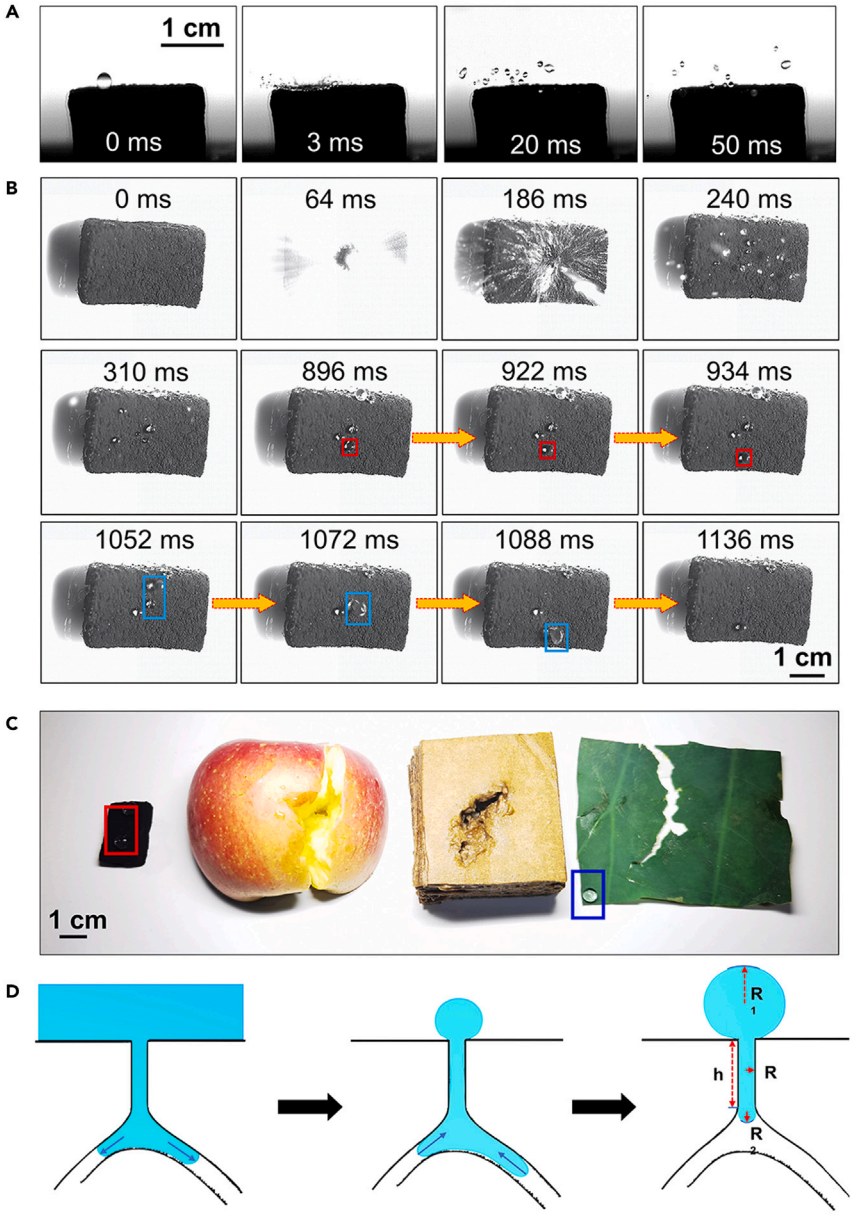

Figure 2. Exceptional high-speed liquid impact resistance

(A) Shows the atomization of water droplets impacting at ~ 4.43 m s^{-1} on our nanocomposites.

(B) Images in top row capture the jet impact test with a speed of ~85.4 m s^{-1}. The middle- and bottom-row images capture water emerging from the nanocomposites at the point of impact and resulting in a growing droplet, which eventually sheds off the surface (see red and blue boxes). The timescale of liquid ejection is O(1)–O(10) s and agrees with a scaling analysis for liquid ejection from hydrophobic pores. The post-impact superhydrophobicity was tested by dropping water droplets at the impact location.

(C) Photos of a nanocomposite sample, an apple, a piece of cardboard, and a lotus leaf after undergoing a similar impact test to elucidate the robustness of our nanocomposites.

(D) Schematic depicting post-impact, capillarity-driven liquid ejection from a pore in our nanocomposite.

Thermal resistance and icephobicity

In applications such as steam condensers or thermal management, the material experiences high temperatures. However, silane coupling agents or some polymers

Please cite this article in press as: Wu et al., Porous bulk superhydrophobic nanocomposites for extreme environments, Matter (2023), https://doi.org/10.1016/j.matt.2023.03.033

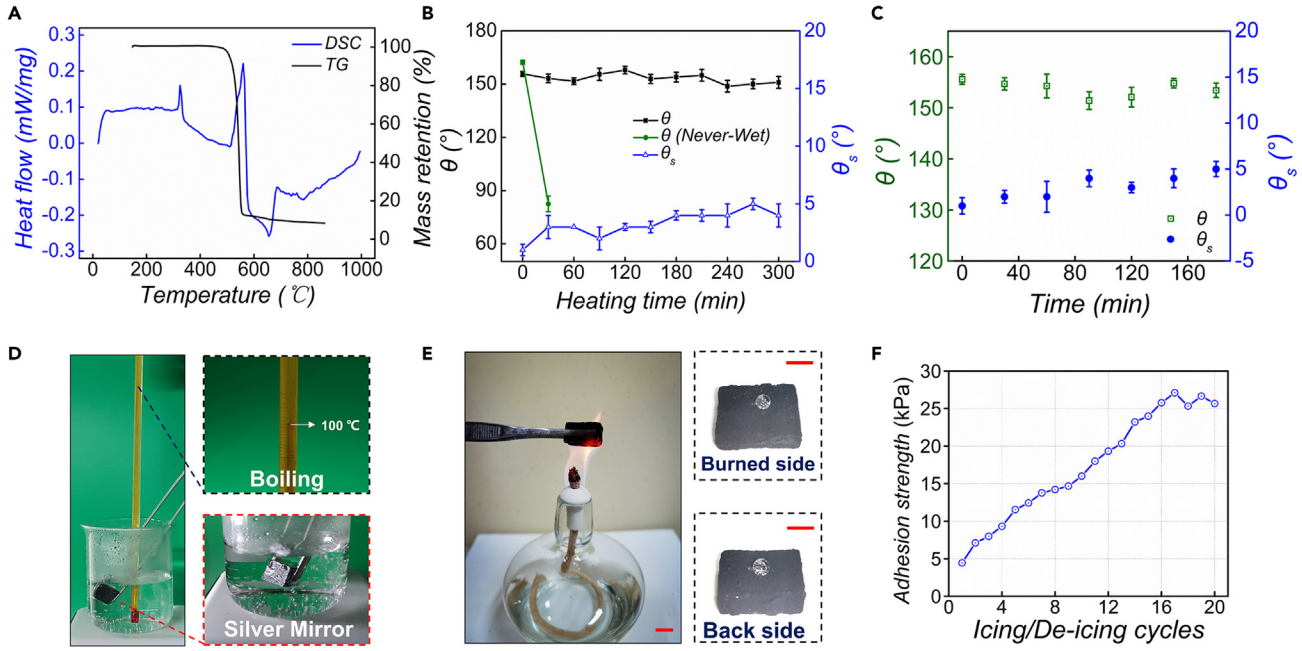

Figure 3. Thermal stability and icephobicity

(A) Results of DSC and TG performed in N_2 for the nanocomposites with 12 wt % CNT.

(B) Effect of heating at 400°C for different durations on wettability; a NeverWet coating sample was also included for comparison.

(C) θ and θ_s measured after immersion in boiling water bath for different times.

(D) Boiling water immersion setup, also capturing the thermometer reading (top inset) and the silver mirror effect (bottom inset) during the test.

(E) Photograph of the sample exposed to an alcohol lamp flame. The specimen shows good flame retardancy. Scale bar, 1 cm.

(F) Effect of icing/de-icing cycles on ice-adhesion strength of the nanocomposites impregnated with PDMS/silicone oil mixture.

typically used in superhydrophobic surface fabrication are susceptible and degrade thermally.[23–25] Thus, thermal stability of the prepared samples was carefully evaluated. First, we performed differential scanning calorimetry (DSC) and thermogravimetry (TG) tests (Figure S4A). The results in a nitrogen atmosphere are shown in Figure 3A and reveal the first endothermic peak of the DSC at ~325°C, which should correspond to the melting point of PTFE, since no mass change is observed in the TG at this temperature.[10] The TG curve begins to decrease at ~480°C, along with a corresponding endothermic peak in DSC. This indicates the decomposition of PTFE, which completes at ~560°C. CNTs cannot react with nitrogen and hence remain intact after high-temperature treatment, leading to ~12 wt % leftover. The results for DSC and TG tests in air (shown in Figure S4B) are similar because PTFE is not sensitive to air either. However, the exothermic DSC peak at ~515°C indicates that CNT is oxidized in air, resulting in the mass retention ratio—the ratio (percentage) of post-abrasion nanocomposite mass to the starting mass—falling to ~0% in the end. To further assess the thermal stability in a more practical way (Video S6), the nanocomposites were heated at 300°C (Figure S4C) and 400°C in air (Figure 3B), followed by cooling down to ambient temperature and measuring the water drop contact angle (θ) and sliding angle (θ_s) after every 30 min of heating. The nanocomposites retain $\theta_s < 5°$ and $\theta > 150°$ even after being heated for 300 min at 400°C. This should be ascribed to the thermostability of the constituents as well as the high viscosity of melt PTFE,[22] which help keep the surface structure intact. For comparison, Figure 3B also includes the data on a popular commercial NeverWet coating treated to 400°C. After being heated for only 30 min, the commercial product quickly lost its superhydrophobicity (see also Figure S4D). To validate superhydrophobicity of the heated sample, besides wettability characterization a water jet impact test at ~20.3 m s^{-1}

Please cite this article in press as: Wu et al., Porous bulk superhydrophobic nanocomposites for extreme environments, Matter (2023), https://doi.org/10.1016/j.matt.2023.03.033

was carried out (Video S7) for confirmation. The test establishes the dynamic liquid repellence for applications requiring high thermal resistance, but there were signs of superficial damage to the nanoporous layer, and hence these samples were not subjected to high-speed impact. Wang et al.[23] prepared a multi-layered superhydrophobic coating with PTFE and a ceramic skeleton, which showed high-temperature resistance of up to 515°C. However, heating PTFE beyond 480°C is extremely harmful because it decomposes and produces hypertoxic gases.[26,27] Besides the remarkable high-speed liquid impact resistance presented above, our nanocomposites also sustain prolonged immersion in boiling water and are flame resistant (presented below). These damage-tolerance capabilities are enabled by the bulk nature and hierarchical porosity of our nanocomposites as opposed to (surface) coatings.

Hot water has lower surface tension, and vapor may also damage superhydrophobicity. In fact, resistance to hot water is not universal for superhydrophobic surfaces.[28–31] Thus, we first measured θ and θ_s at temperatures from 20°C to 100°C. The results are plotted in Figure S5A and show that our nanocomposites can maintain superhydrophobicity even with hot water. However, this test is not harsh enough because the water temperature will naturally start decreasing immediately after being placed on the surfaces and during the course of wettability tests. Thus, for a harsher test, we immersed the samples in boiling water (Video S8). The effect of immersion time on the wettability is shown in Figure 3C. Clearly, θ is maintained above 150° and θ_s at ~5° after 180 min of immersion in boiling water. Moreover, the post-immersion morphology of samples (Figure S5B) remained unchanged. The boiling water immersion test shown in Figure 3D clearly shows the silver mirror phenomenon on the specimen's surface attesting to its Cassie-state superhydrophobicity. Owing to the excellent boiling water repellence, water vapor only accumulates on the surface of the sample to form a gas film rather than invading the microstructure and causing surface wetting.[32] Next, the sample was exposed to an alcohol lamp flame (Figure 3E). The outer flame of the alcohol lamp can reach 600°C, but even in this condition only a small part of the surface was burned red and was able to prevent further combustion. Also, after the test the burned surface still maintained superhydrophobicity (Video S9).

Ice accretion is a problem for much outdoor equipment. The ice-adhesion strength on as-prepared, porous superhydrophobic nanocomposites was 33.63 $\pm$ 5.12 kPa, which confirms their icephobicity[33] (see Figures S6A and S6B). The porous structure of the nanocomposites also enabled us to impregnate them with a mixture of polydimethylsiloxane (PDMS) and silicone oil to achieve long-lasting icephobicity with low ice-adhesion strength (Note S4). Figure 3F presents the effect of icing/de-icing cycles on ice-adhesion strength. Owing to the low surface energy and interfacial toughness of PDMS/silicone oil mixture, we measured the ice-adhesion strength as 4.4 kPa, which is well below the 10 kPa required for ready dislodgment of ice from surfaces.[34] Additionally, the adhesion strength only crept up to ~25 kPa after 20 icing/de-icing cycles.

Mechanochemical robustness

Particle collision is inevitable in real-life applications such as outdoor infrastructure or transport systems. Particle impact can alter the surface topography, and often the surface chemistry. Thus, the nanocomposites were tested using the setup depicted in Figure S7A. The sand container was 30 cm above the specimens, which were tilted by 45° (Figure S7A). The SiO_2 particles in the sand were sized between 355 and 710 μm. After 4,200 g of sand impacted, θ remained above 150° while θ_s increased from 1° to 9° (Figure 4A).

Please cite this article in press as: Wu et al., Porous bulk superhydrophobic nanocomposites for extreme environments, Matter (2023), https://doi.org/10.1016/j.matt.2023.03.033

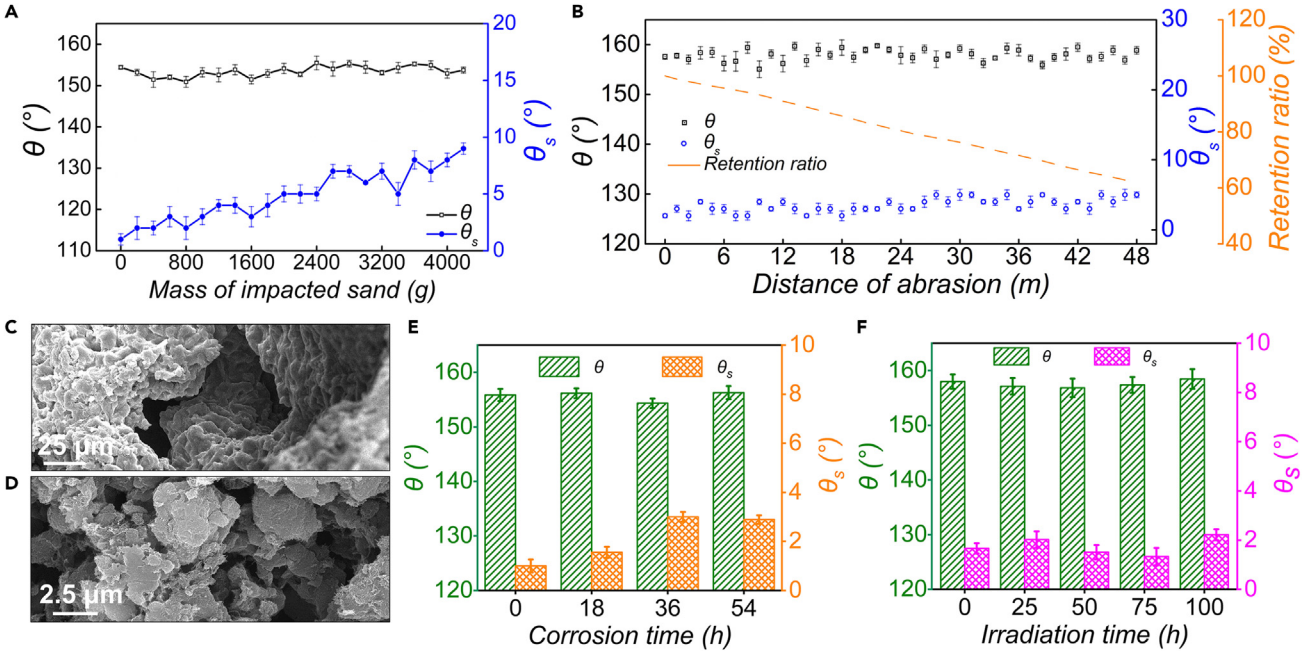

Figure 4. Mechanochemical robustness and UV stability

(A) Effect of impacted sand's total weight on the wettability.

(B) Effect of abrasion distance on the wettability of the prepared specimens, tested with an 80-grit sandpaper and ~5 kPa pressure.

(C and D) SEM images of the samples after the sand impact test (C) and sandpaper abrasion (D).

(E) Change of θ and θ_s after different durations of immersion in aqua regia.

(F) Change of θ and θ_s after different durations of exposure to high-intensity UV light.

Next, a standard linear abrasion setup was used to abrade the surfaces with loaded sandpaper (80 grit) with ~5 kPa pressure (Figure S7B). In Figure 4B the θ, θ_s, and retention ratio are plotted against abrasion distance. After an abrasion distance of 60 m, the surface retains excellent water repellence with a retention ratio of 52%. Furthermore, the θ_s, which is generally more sensitive to mechanical damage than θ,[35] stabilized at ~5°. The surface morphology of a sample after the sand impact test and the abrasion test, presented in Figures 4C and 4D, respectively. Clearly the micro-/nanoscale hierarchy is retained, although some flattening is also observed, as reflected in the modest rise in θ_s. Another reason for this good wear resistance should lie in the constituents selected, which endow our nanocomposites with a rather low friction coefficient of ~0.08 (cf. Figure S8 and Note S5). For a more complete understanding, the samples were also tested with finer sandpapers (360 grit and 600 grit) and larger abrasion pressures (~10 kPa and ~15 kPa). The results for 360-grit and 600-grit sandpaper abrasion (with pressure of ~5 kPa) are presented in Figures S7C and S7D, respectively. The finer-grit abrasion tests were only run for 12 m to gain an impression of the changes. Abrasion tests with different pressures (using 80-grit sandpaper) also have similar results, with both θ and θ_s remaining within the threshold of superhydrophobicity (Figures S7F and S7G). The retention ratios for different abradants and pressures are plotted in Figures S7E and S7H. Clearly, rougher abradants (lower grit size) and higher pressures cause larger mass loss. It can be also concluded that abrasion pressure had a larger effect than abradant roughness, since after being abraded by 15 kPa pressure for 12 m, the retention ratio dropped to 62%. Furthermore, we utilized additional practical ways to test the abrasion resistance of the sample (Videos S10, S11, S12, and S13), such as file abrasion and steel wool abrasion (for even harsher abrasion under water, see Videos S14 and S15).

Please cite this article in press as: Wu et al., Porous bulk superhydrophobic nanocomposites for extreme environments, Matter (2023), https://doi.org/10.1016/j.matt.2023.03.033

The ability to retain the composite air/liquid interface also enables superhydrophobic surfaces to be chemically resistant. However, many ingredients limit the surfaces in applications involving severely corrosive chemicals, e.g., aqua regia or high-concentration alkalis. Our choice of PTFE lends excellent advantage to this end. We used aqua regia and 5 M sodium hydroxide (NaOH) solution to evaluate the chemical robustness of our nanocomposites. After immersing in aqua regia for 54 h or 5 M NaOH solution for 48 h (see Figures 4E and S9C, respectively), the sample was still superhydrophobic with θ_s less than 5°. The surface morphology (Figure S9) shows no discernible change with respect to the pristine counterparts.

UV exposure is inevitable in outdoor conditions. We employed a UV source with an intensity of 6.82 W/m^2 (about four times that of sunlight) to test our samples (Figure 4F). After 100 h, the nanocomposites retained superhydrophobicity.

Last but not least, using different shapes/sizes of the PU sponges, our bulk nanocomposites can be fabricated into different shapes such as a hollow pipe, a cube, and a triangular prism (Figure S10 and Note S6).

To compare against previously reported superhydrophobic materials, we collected data on linear abrasion, chemical corrosion, sand impact test, water jet impact, and high-temperature resistance results for different superhydrophobic bulk components, coatings, and films reported in the literature. We also applied the same series of tests on a popular commercial superhydrophobic coating such as NeverWet (Note S7). Table S1 shows the result of this exercise. Compared with these previous reports, our bulk nanocomposites (with 12 wt % CNT) show a clear all-round improvement.

Conclusions

In summary, we introduced a new templated approach to the manufacture of bulk superhydrophobic nanocomposites with mechanochemical robustness suitable for a diversity of extreme conditions. The nanoscale channels on the surface as well as the porous structure inside the bulk nanocomposite enabled them to resist water jets with velocities up to ~85.4 m s^{-1} (i.e., well into category 5 hurricane speed thresholds). With their rationally selected ingredients, our nanocomposites could also retain superhydrophobicity after being heated at 400°C, immersion in boiling water for 180 min, or exposure to an alcohol flame. In addition, our nanocomposites, with a hierarchically porous and CNT reinforced microstructure, show excellent resistance to long-distance mechanical abrasion, long-term immersion in highly corrosive media such as aqua regia and sodium hydroxide solution, or UV exposure. Furthermore, the surfaces were icephobic, and their icephobicity could be enhanced by impregnating them with a PDMS/silicone oil mixture. These nanocomposites may serve applications in severe industrial fileds or under harsh weather conditions, which have so far proved elusive to superhydrophobic materials.

EXPERIMENTAL PROCEDURES

Resource availability

Lead contact

Further information and requests for resources and reagents should be directed to and will be fulfilled by the lead contact, Manish K. Tiwari, at m.tiwari@ucl.ac.uk.

Materials availability

This study did not generate new unique reagents.

Data and code availability

All experimental data supporting the findings of this paper are available from the corresponding authors upon reasonable request.

Preparation of porous superhydrophobic CNT/PTFE nanocomposites

Superhydrophobic nanocomposites were prepared using a foam template infusion and sintering process, as shown schematically in Figure 1. First, CNT (average diameters of 4–6 nm; Chengdu Organic Chemicals, China) and PTFE nanoparticles (average diameters of 200 nm; Aladdin, China) were mixed in ethanol (Aladdin) in different ratios. The mixture was subjected to sonication for 20 min and high-speed shearing at 10,000 rpm for 20 min to prevent aggregation. Thereafter, the PU foam (Hongsiyuan Special Foam Material, China) was immersed in the suspension to infuse it with the mixed fillers and heated at 80°C for 30 min. The process was repeated several times to complete the foam loading and to ensure that an excess accretion layer of nanoparticles was formed on the fully infused sponge. Finally, the infused foam was sintered at 390°C for 2 h to degrade the PU away and create the porous superhydrophobic nanocomposites with a hierarchical porous structure, featuring fine (nanoscale) pores on the surface connected to larger (microscale) porosity in the sample interior. To analyze the effects of CNT, superhydrophobic nanocomposite foams containing 4 wt %, 8 wt %, 12 wt %, 16 wt %, 20 wt %, and 24 wt % CNT were fabricated. The PU sponge template could be given many different shapes and was used to make special-shaped products, such as blocks, pipe fittings, and pentagonal stars.

Characterization and instruments

Surface morphology of the prepared samples was evaluated by SEM. A field emission gun scanning electron microscope (Tescan Maia 3, Czechia) was used in high-vacuum mode and with a working voltage of 15 kV. Before observation, thin gold films were sputtered on all samples by using a low-conductivity sputtering coater (SC7620; Quorum, UK) for 200 s in a vacuum with a current of 15 mA. An FTIR spectroscope (FTIR-1500, China) was used to analyze chemical composition via a KBr pellet method in the wavenumber range of 4,000–500 cm^{-1}. Water droplet contact (denoted by θ) and sliding (denoted by θ_s) angles were measured using a contact angle meter (SL200B; Solon, China). For each surface sample, θ was measured at least at three different locations, and ~5-μL deionized water droplets were used. The water droplets were kept on the surface for at least 20 s before the measurement. The mechanical property was evaluated by a SANS (China) universal tester at a displacement rate of 1 mm/min. Linear friction measurements were carried out with a friction-testing machine. The loading force was 10 N and the rotating speed 50 rpm. DSC and TG analyses were carried out in N_2 and air, with an STA 449 F5 Jupiter simultaneous thermal analyzer (Netzsch, Selb, Germany) at a heating rate of 5°C/min.

SUPPLEMENTAL INFORMATION

Supplemental information can be found online at https://doi.org/10.1016/j.matt.2023.03.033.

ACKNOWLEDGMENTS

N.W. acknowledges the research project of NUDT, ZK20-08, and Hunan Provincial Natural Science Foundation of China (2021JJ30028). C.P. acknowledges support by the National Natural Science Foundation of China (no. 51203183) and the Science and Technology Innovation Program of Hunan Province (2020RC4037). M.K.T.

acknowledges the Royal Society Wolfson Fellowship and the NICEDROPS project supported by the European Research Council under the European Union's Horizon 2020 research and innovation program under grant agreement no. 714712.

AUTHOR CONTRIBUTIONS

B.W., C.P., and M.K.T. conceived the superhydrophobic nanocomposites for extreme environments presented. C.P. and M.K.T. guided the work with assistance from N.W., and B.W., C.P., and M.K.T. planned the experiments. B.W. and Y.M. executed all of the experiments, with support from N.W. and S.X. on nanocomposite fabrication process and Jinshui Yang and C.Y. on water jet impact experimental setup. B.W., C.P., and M.K.T. wrote the paper and interpreted the results, with constructive comments from Y.M., N.W., Jun Yang, and S.B.

DECLARATION OF INTERESTS

M.K.T. is engaged in potential commercialization of a few coatings formulations, which are superhydrophobic. M.K.T. is a scientific advisor in two small companies, AcousticaBio (registered in the USA) and Medoron (registered in the UK). M.K.T. is co-inventor of several patents and applications on superhydrophobic materials.

Received: August 6, 2021
Revised: January 13, 2023
Accepted: March 29, 2023
Published: April 20, 2023

REFERENCES

1. Lafuma, A., and Quéré, D. (2003). Superhydrophobic states. Nat. Mater. *2*, 457–460.
2. Li, X., Yang, J., Lv, K., Papadopoulos, P., Sun, J., Wang, D., Zhao, Y., Chen, L., Wang, D., Wang, Z., and Deng, X. (2021). Salvinia-like slippery surface with stable and mobile water/air contact line. Natl. Sci. Rev. *8*, nwaa153.
3. Wang, D., Sun, Q., Hokkanen, M.J., Zhang, C., Lin, F.-Y., Liu, Q., Zhu, S.P., Zhou, T., Chang, Q., He, B., et al. (2020). Design of robust superhydrophobic surfaces. Nature *582*, 55–59.
4. Peng, C., Chen, Z., and Tiwari, M.K. (2018). All-organic superhydrophobic coatings with mechanochemical robustness and liquid impalement resistance. Nat. Mater. *17*, 355–360.
5. Vasileiou, T., Gerber, J., Prautzsch, J., Schutzius, T.M., and Poulikakos, D. (2016). Superhydrophobicity enhancement through substrate flexibility. Proc. Natl. Acad. Sci. USA *113*, 13307–13312.
6. Luo, H., Yang, M., Li, D., Wang, Q., Zou, W., Xu, J., and Zhao, N. (2021). Transparent super-repellent surfaces with low haze and high let impact resistance. ACS Appl. Mater. Interfaces *13*, 13813–13821.
7. Tang, Y., Yang, X., Li, Y., Lu, Y., and Zhu, D. (2021). Robust micro-nanostructured superhydrophobic surfaces for long-term dropwise condensation. Nano Lett. *21*, 9824–9833.
8. Sun, M., Boo, C., Shi, W., Rolf, J., Shaulsky, E., Cheng, W., Plata, D.L., Qu, J., and Elimelech, M. (2019). Engineering carbon nanotube forest superstructure for robust thermal desalination membranes. Adv. Funct. Mater. *29*, 1903125–1903137.
9. Lambley, H., Schutzius, T.M., and Poulikakos, D. (2020). Superhydrophobic surfaces for extreme environmental conditions. Proc. Natl. Acad. Sci. USA *117*, 27188–27194.
10. Das, I., and De, G. (2015). Zirconia based superhydrophobic coatings on cotton fabrics exhibiting excellent durability for versatile Use. Sci. Rep. *5*, 18503–18513.
11. Li, Y., Hu, T., Li, B., Wei, J., and Zhang, J. (2019). Totally waterborne and highly durable superamphiphobic coatings for anti-icing and anticorrosion. Adv. Mater. Interfac. *6*. 1901255–1901234.
12. Mouterde, T., Lecointre, P., Lehoucq, G., Checco, A., Clanet, C., and Quéré, D. (2019). Two recipes for repelling hot water. Nat. Commun. *10*, 1410–1416.
13. Smirnov, S., Vlassiouk, I., Takmakov, P., and Rios, F. (2010). Water confinement in hydrophobic nanopores. pressure-induced wetting and drying. ACS Nano *4*, 5069–5075.
14. Washburn, E.W. (1921). The dynamics of capillary flow. Phys. Rev. *17*, 273–283.
15. An, A.K., Guo, J., Lee, E.-J., Jeong, S., Zhao, Y., Wang, Z., and Leiknes, T. (2017). PDMS/PVDF hybrid electrospun membrane with superhydrophobic property and drop impact dynamics for dyeing wastewater treatment using membrane distillation. J. Membr. Sci. *525*, 57–67.
16. Zhu, X., Zhang, Z., Ren, G., Yang, J., Wang, K., Xu, X., Men, X., and Zhou, X. (2012). A novel superhydrophobic bulk material. J. Mater. Chem. *22*, 20146–20148.
17. Donati, M., Lam, C.W.E., Milionis, A., Sharma, C.S., Tripathy, A., Zendeli, A., and Poulikakos, D. (2020). Sprayable thin and robust carbon nanofiber composite coating for extreme jumping dropwise condensation performance. Adv. Mater. Interfac. *8*, 2001176–2001186.
18. Delogu, L.G., Vidili, G., Venturelli, E., Ménard-Moyon, C., Zoroddu, M.A., Pilo, G., Nicolussi, P., Ligios, C., Bedognetti, D., Sgarrella, F., et al. (2012). Functionalized multiwalled carbon nanotubes as ultrasound contrast agents. Proc. Natl. Acad. Sci. USA *109*, 16612–16617.
19. Deng, X., Mammen, L., Butt, H.J., and Vollmer, D. (2012). Candle soot as a template for a transparent robust superamphiphobic coating. Science *335*, 67–70.
20. Maitra, T., Tiwari, M.K., Antonini, C., Schoch, P., Jung, S., Eberle, P., and Poulikakos, D. (2014). On the nanoengineering of superhydrophobic and impalement resistant surface textures below the freezing temperature. Nano Lett. *14*, 172–182.
21. Wang, Y., Xue, J., Wang, Q., Chen, Q., and Ding, J. (2013). Verification of icephobic/anti-icing properties of a superhydrophobic surface. ACS Appl. Mater. Interfaces *5*, 3370–3381.
22. Maitra, T., Antonini, C., Tiwari, M.K., Mularczyk, A., Imeri, Z., Schoch, P., and Poulikakos, D. (2014). Supercooled water drops impacting

superhydrophobic textures. Langmuir *30*, 10855–10861.

23. Wang, S., Wang, Y., Zou, Y., Chen, G., Ouyang, J., Jia, D., and Zhou, Y. (2020). Scalable-manufactured superhydrophobic multilayer nanocomposite coating with mechanochemical robustness and high-temperature endurance. ACS Appl. Mater. Interfaces *12*, 35502–35512.

24. Zhu, K., Zhang, J., Zhang, H., Tan, H., Zhang, W., Liu, Y., Zhang, H., and Zhang, Q. (2018). Fabrication of durable superhydrophobic coatings based on a novel branched fluorinated epoxy. Chem. Eng. J. *351*, 569–578.

25. Cheng, Y., Zhu, T., Li, S., Huang, J., Mao, J., Yang, H., Gao, S., Chen, Z., and Lai, Y. (2019). A novel strategy for fabricating robust superhydrophobic fabrics by environmentally-friendly enzyme etching. Chem. Eng. J. *355*, 290–298.

26. Conesa, J.A., and Font, R. (2001). Polytetrafluoroethylene decomposition in air and nitrogen. Polym. Eng. Sci. *41*, 2137–2147.

27. Purser, D.A. (1992). Recent developments in understanding the toxicity of PTFE thermal decomposition products. Fire Mater. *16*, 67–75.

28. Zhang, X.F., Zhao, J.P., and Hu, J.M. (2017). Abrasion-resistant, hot water-repellent and self-cleaning superhydrophobic surfaces fabricated by electrophoresis of nanoparticles in electrodeposited sol-gel films. Adv. Mater. Interfac. *4*, 1700177–1700184.

29. Zhang, J., Yu, B., Gao, Z., Li, B., and Zhao, X. (2017). Durable, transparent, and hot liquid repelling superamphiphobic coatings from polysiloxane-modified multiwalled carbon nanotubes. Langmuir *33*, 510–518.

30. Wu, Y., Jia, S., Wang, S., Qing, Y., Yan, N., Wang, Q., and Meng, T. (2017). A facile and novel emulsion for efficient and convenient fabrication of durable superhydrophobic materials. Chem. Eng. J. *328*, 186–196.

31. Li, B., and Zhang, J. (2016). Durable and self-healing superamphiphobic coatings repellent even to hot liquids. Chem. Commun. *52*, 2744–2747.

32. Guo, F., Wen, Q., Peng, Y., and Guo, Z. (2017). Simple one-pot approach toward robust and boiling-water resistant superhydrophobic cotton fabric and the application in oil/water separation. J. Mater. Chem. *5*, 21866–21874.

33. Golovin, K., Kobaku, S.P.R., Lee, D.H., DiLoreto, E.T., Mabry, J.M., and Tuteja, A. (2016). Designing durable icephobic surfaces. Sci. Adv. *2*, e1501496.

34. Zhuo, Y., Xiao, S., Håkonsen, V., Li, T., Wang, F., He, J., and Zhang, Z. (2020). Ultrafast self-healing and highly transparent coating with mechanically durable icephobicity. Appl. Mater. Today *19*, 100542–100553.

35. Li, Y., Li, B., Zhao, X., Tian, N., and Zhang, J. (2018). Totally waterborne, nonfluorinated, mechanically robust, and self-healing superhydrophobic coatings for actual anti-icing. ACS Appl. Mater. Interfaces *10*, 39391–39399.